Protein expression in the obligate hydrocarbon-degrading psychrophile Oleispira antarctica RB-8 during alkane degradation and cold tolerance

Gregson, Benjamin H.; Metodieva, Gergana; Metodiev, Metodi V.; Golyshin, Peter; McKew, Boyd A.

Environmental Microbiology

Published: 01/05/2020

Peer reviewed version

Title: Protein expression in the obligate hydrocarbon-degrading psychrophile *Oleispira antarctica* RB-8 during alkane degradation and cold tolerance.

Authors: Benjamin H. Gregson[a], Gergana Metodieva[a], Metodi V. Metodiev[a], Peter N. Golyshin[b,c], Boyd A. McKew[a]

Affiliations: [a]School of Biological Sciences, University of Essex, Colchester, Essex, CO4 3SQ, UK

[b]School of Natural Sciences, College of Environmental Sciences and Engineering, Bangor University, Bangor, UK

[c] Centre for Environmental Biotechnology, Bangor University, Deiniol Rd, Bangor LL57 2UW, UK

Running Title: Proteomes of alkane-degrading *O. antarctica* RB-8

Corresponding Author: Boyd A McKew, School of Biological Sciences, University of Essex, Colchester, Essex, CO4 3SQ UK.

Tel: +44 (0) 1206 873010

Fax: +44 (0) 1206 872592

Email: boyd.mckew@essex.ac.uk

Originality significance statement

Hydrocarbon degradation is affected by temperature due to the solubility and accessibility of substrates to microbes. The largest habitat for microbes on Earth is the ocean and >90% of it is at or below 4°C. *Oleispira antarctica* RB-8 is a marine psychrophilic obligate hydrocarbon-degrader that dominates microbial communities at lower temperatures following oil pollution events, or the addition of hydrocarbons into water. Despite the important role *O. antarctica* plays in natural attenuation of cold oil-contaminated marine environments proteomic analysis during hydrocarbon degradation or cold tolerance has not previously been presented. This is the first study to characterise the difference in the proteome of *O. antarctica* during growth on alkanes versus a non-hydrocarbon control highlighting key enzymes involved in hydrocarbon degradation. It also investigates temperature-dependent changes in the proteome to find mechanisms of cold tolerance which could provide *O. antarctica* with competitive advantages over other hydrocarbon-degrading bacteria.

Summary

In cold marine environments the obligate hydrocarbon-degrading psychrophile *Oleispira antarctica* RB-8, which utilizes aliphatic alkanes almost exclusively as substrates, dominates microbial communities following oil spills. In this study, LC-MS/MS shotgun proteomics was used to identify changes in the proteome induced during growth on *n*-alkanes and in cold temperatures. Specifically, proteins with significantly higher relative abundance during growth on tetradecane (*n*-C_{14}) at 16°C and 4°C have been quantified. During growth on *n*-C_{14}, *O. antarctica* expressed a complete pathway for the terminal oxidation of *n*-alkanes including two alkane monooxygenases, two alcohol dehydrogenases, two aldehyde dehydrogenases, a fatty-acid-CoA ligase, a fatty acid desaturase and associated oxidoreductases. Increased biosynthesis of these proteins ranged from 3-fold to 21-fold compared to growth on a non-hydrocarbon control. This study also highlights mechanisms *O. antarctica* may utilise to provide it with ecological competitiveness at low temperatures. This was evidenced by an increase in spectral counts for proteins involved in flagella structure/output to overcome higher viscosity, flagella rotation to accumulate cells, and proline metabolism to counteract oxidative stress, during growth at 4°C compared to 16°C. Such species-specific understanding of the physiology during hydrocarbon degradation can be important for parametrising models that predict the fate of marine oil spills.

Introduction

Oleispira antarctica RB-8 is a psychrophilic aerobic bacterium belonging to the Gammaproteobacteria class, which was first isolated from oil-enriched microcosms containing seawater from Rod Bay (Ross Sea, Southern Antarctica) (Yakimov *et al.*, 2003). *O. antarctica* is a member of a group of organisms known as obligate hydrocarbonoclastic bacteria (OHCB) which grow on a highly restricted spectrum of substrates, predominantly aliphatic hydrocarbons. Oil pollution in marine environments rapidly induces a bloom of OHCB which can constitute up to 80-90% of the microbial community (Harayama et al., 1999; Kasai et al., 2002). *Oleispira* shares many traits with other described genera of marine OHCB, such as *Alcanivorax* (Yakimov *et al.*, 1998) and *Thalassolituus* (Yakimov *et al.*, 2004) including their marine origin, purely respiratory metabolism, and the capability of growth almost exclusively on aliphatic alkanes and their derivatives. However, in contrast with these genera, which contain species that are characterized by mesophilic behaviour, *O. antarctica* has a broad growth temperature optimum between 1 and 15°C (Yakimov *et al.*, 2003). The minimal growth temperature is estimated to be -6.8°C using the Ratkowsky square-root temperature growth model (Ratkowsky *et al.*, 1983). Around 90% of the biosphere exists at temperatures below 10°C and this provides ample opportunity for *Oleispira* spp. to dominate microbial communities due to their ecological competitiveness in cold environments (Feller and Gerday, 2003; Hazen et al, 2010; Mason et al, 2012; Kube et al, 2013).

The GenBank and RDP databases contain 16S rRNA gene sequences of 25 *Oleispira* bacteria originating from microbial communities from cold environments such as Arctic sea ice (Gerdes *et al.*, 2005; Brakstad *et al.*, 2008), sediments (Dong *et al.*, 2015) and an epishelf lake (Veillette et al., 2011), Antarctic and subantarctic seawater (Prabagaran et al., 2007; Singh et al., 2015), and seawater from the Norwegian fjord Trondheimsfjord (Brakstad and Bonaunet, 2006), and the Irish and North Seas (Coulon et al., 2007; Gertler et al., 2012,). Warmer locations include fish farm sediments in Southern Tasmania (Bissett et al., 2006), marine basalts from the East Pacific Rise (Mason et al., 2007) and coastal seawater (Wang et al., 2012).

Previous reports have shown that *Oleispira* species can be among the most dominant community members in the presence of aliphatic petroleum hydrocarbons at lower temperatures and can outcompete other OHCB such as *Thalassolituus* (Coulon et al.,2007), or *Alcanivorax*, which is often the most dominant alkane degrader in marine oil spills (Harayama *et al.*, 2004; Kostka *et al.*, 2011). For example, bacteria related to *O. antarctica* (98% 16S rRNA similarity) became the most dominant bacteria in crude-oil amended North Sea Thames Estuary microcosms incubated at 4°C, in contrast to microcosms incubated at 20°C where the abundance of *Thalassolituus* was highest (Coulon *et al.*, 2007). *Oleispira* were also found to be predominant in cold deep-water samples (Depth-1099 to 1219m, average temperature 4.7°C) after the Deepwater Horizon oil spill in the Gulf of Mexico (Hazen *et al.*, 2010; Mason *et al.*, 2012). Furthermore, *Oleispira* sequences were present at a high abundance (14-17% of recovered reads) in 16S rRNA gene libraries of oil-enriched microcosms from the Gulf at Mexico grown at 5° (Techtmann *et al.*, 2017).

The genome sequencing of *O. antarctica* RB-8 revealed an array of genes putatively involved in adaption to cold environments such as chaperonins, Cpn60 (C29610) and Cpn10 (C29620), which can reduce the maximum growth temperature of mesophiles (Ferrer et al., 2003; Kube et al., 2013). Analysis of the chaperonin interactome suggest that protein-chaperone interactions are protecting functionality of proteins at low temperatures (Strocchi et al., 2006; Kube et al., 2013). The genome sequencing also revealed putative genes for hydrocarbon degradation including three alkane monooxygenase and one P450 cytochrome gene. The first alkane monooxygenase gene (C23040) has its closest homologue in AlkB2 from *A. borkumensis* SK2 and is also encoded next to the transcriptional regulator GntR. Two other alkane monooxygenases (C34350 and C34450) are clustered within putative operons (C34330-C34360 and C34430-C4450, respectively) both with genes that code for a transcriptional regulator of the AraC family and an oxidoreductase The first operon also containsan alcohol dehydrogenase (C34360) which is similar to the alcohol dehydrogenase AlkJ from *A. borkumensis* SK2. Greater mRNA expression of these genes in *O. antarctica* was quantified during growth on tetradecane (*n*-C_{14}) (compared to the non-hydrocarbon substrate acetate) through

targeted quantitative reverse transcription polymerase chain reaction (Kube et al., 2013). However, mRNA abundance was only calculated for three *alkB* genes and one *P450* gene. To date their translation has not been confirmed at the protein level and no study has compared expression of either a total transcriptome or shotgun proteome in *O. antarctica* during growth on alkanes versus a non-hydrocarbon control or at different temperatures. Comparing protein expression during growth on a petroleum hydrocarbon versus a non-hydrocarbon substrate will enable us to see the compositional and abundance changes within the total proteome to identify the key enzymes involved in the metabolism of these crude oil components. By measuring the proteomic response at different temperatures, we can also understand potential mechanisms *O. antarctica* uses which provides it ecological competitiveness over other hydrocarbon-degrading bacteria and why it regularly dominates oil-contaminated environments at low temperatures. Such bottom-up experimental approaches that yield a species-specific understanding of hydrocarbon degradation can be important for parametrising future improved models that predict the biodegradative fate of marine oil spills by complex microbial communities (Röling and van Bodegom, 2014). There is a growing interest in post-spill monitoring of microbial communities (Kirby et al., 2018) and an understanding of the key proteins involved in hydrocarbon degradation is important for designing gene primers that can be used in monitoring tools that are based on the abundance of specific functional genes. This can complement current tools based on community 16S rRNA genes, such as the Ecological Index of Hydrocarbon Exposure (Lozada et al., 2014).

In this study, we used LC-MS/MS shotgun proteomics, to identify changes in the proteome induced during growth on alkanes and at cold temperatures. Specifically, proteins with significant increases in spectral counts during growth on *n*-C_{14} at 16°C and 4°C have been quantified, giving a unique insight in the proteins involved in the degradation of alkanes and cold adaptation.

Results

Growth on alkanes: Preliminary growth tests to determine the alkane degradation range of *O. antarctica* RB-8 were performed with alkanes in the size range from 10 carbons atoms (decane) to 32 carbon atoms (dotriacontane) including *n*-C_{10}, *n*-C_{12}, *n*-C_{16}, *n*-C_{20}, *n*-C_{24}, *n*-C_{28} and *n*-C_{32} and the branched alkane pristane (2,6,10,14-tetramethylpentadecane) with the degradation of these compounds confirmed and quantified through GC-MS analysis. *O. antarctica* RB-8 grew rapidly at both 4°C or 16°C on *n*-alkanes from *n*-C_{10} to *n*-C_{24} after a 3-day lag phase but was unable to grow on the larger *n*-alkanes or on the branched alkane pristane (no growth was observed after 21-day incubation) (Fig S1). There was no significant difference of growth rates between substrates or temperature (Table S1). Endpoint GC-MS analysis revealed significant ($P<0.05$) alkane degradation in all single substrate microcosms up to *n*-C_{24} after 21 days ranging from 42% to 81% with no significant differences after growth at 4°C or 16°C (Fig S2). Differences in the proteomes were quantified cells growing at either 4°C or 16°C on the medium-chain *n*-alkane tetradecane (*n*-C_{14}), which *O. antarctica* was originally isolated on (Yakimov et al., 2003), versus cells growing on the non-hydrocarbon control Tween 80 (one of the very few non-hydrocarbon substrates OHCB can utilise).

Proteomic overview: A total of 14,8648 spectra were assigned to 1,246 proteins (average of 12,387 spectral counts per replicate and ranging from 1 to 4,772 spectral counts per protein), representing detection of simultaneous expression of ~32% of the total genome that contains 3,919 protein coding genes (Table S2). The effect of both growth substrate and temperature led to expression of differing proteomes for each treatment, with highly similar proteomes observed between the biological replicates (Fig 1A). The vast majority of detected proteins were expressed in highly similar abundance regardless of growth substrate or temperature, with a smaller subset of proteins differing in their expression ratio (Fig 1BCD). Overall 286 were significantly differentially expressed across all 4 treatments (Table S2). A total of 84 proteins were significantly differentially expressed because of the growth substrate, of which 31 proteins showed significant increases in biosynthesis when growing on

167 *n*-C_{14} (Fig 1C). A similar amount of proteins (95) were differentially expressed due to temperature (T_{opt}-
168 1-15°C), with the relative abundance of 47significantly increasing at the cold temperature of 4°C (Fig
169 1D).

170

171 **Alkane induced proteins:** Of the proteins with increased biosynthesis during growth on *n*-C_{14}, many
172 were identified by sequence homology as having specific functions in the hydrocarbon degradation
173 pathway (Fig 2). Two alkane monooxygenases had higher spectral counts during growth on *n*-C_{14}
174 (UniProt ID's R4YQX3 and R4YQY4; Fig. 2). These proteins are required for the first and rate-limiting
175 step of alkane degradation, the introduction of an oxygen atom converting the *n*-alkane into a
176 primary alcohol. The genes coding for these two monooxygenases (C34350 and C34450) are part of
177 gene cassettes (C34330-C34360 and C34430-C34450) which are situated outside the predicted
178 genomic islands and contain genes that code for transcriptional regulators of the AraC family
179 (Gallegos et al., 1997), oxidoreductases, alkane monooxygenases and an alcohol dehydrogenase. The
180 alkane monooxygenase R4YQX3 (coded by C34350) had increased biosynthesis together with AlkJ an
181 alcohol dehydrogenase R4YRA7, coded by the adjacent gene C34360) (Fig. 2). Another alkane-1-
182 monoxygenase (R4YQY4; coded by the gene C34450) was the most abundantly detected alkane
183 monooxygenase and the spectral count was significantly 12-fold higher during growth on *n*-C_{14} along
184 with an oxidoreductase (R4YRS0) coded by the adjacent gene (C34440) which was 21-fold higher
185 (Fig. 2). Domain analysis revealed a 2Fe-2S iron-sulfur cluster binding domain and the protein is a
186 member of the Fer2 (PF00111) family, suggesting it is a ferredoxin.

187 The AlkJ (R4YRA7/C34360) protein, which was exclusively detected during growth on *n*-C_{14} and
188 co-expressed with the alkane monooxygenase (R4YQX3/C34350) is required for the second step of
189 alkane degradation, which is the dehydrogenation of the primary alcohol to yield an aldehyde.
190 Another alcohol dehydrogenase (R4YJ92) also showed increased biosynthesis during growth on the *n*-
191 alkane. This protein, whose spectral count was nine-fold higher during growth on *n*-C14, is coded by

192 the gene C00500 that is part of a putative operon which also contains genes that code for an
193 uncharacterised protein with a signal sequence twin-arginine motif (R4YJC5/C00510), an aldehyde
194 dehydrogenase (R4YMB5/C00520) and a transcriptional regulator (R4YPZ8/C00530).

195 The third step in the alkane degradation pathway is the oxidation of the aldehyde, and two
196 aldehyde dehydrogenases, coded by genes at separate loci (C00520 and C11600), that could putatively
197 catalyse this reaction, had significantly higher spectral counts (Fig. 2). The first (R4YMB5) was
198 approximately four-fold more abundant during growth on *n*-C_{14}, contains an aldehyde dehydrogenase
199 activity domain (pfam00171) and is NAD(P) dependent. The second aldehyde dehydrogenase (R4YL03)
200 also had approximately a six-fold higher spectral count during growth on *n*-C_{14}.

201 The oxidation of the aldehyde yields a complex fatty acid and proteins involved in their
202 catabolism which showed increased biosynthesis included a medium-chain fatty acid CoA ligase
203 (R4YKT2/C09310; 3-fold higher spectral counts) involved in the activation of the fatty acid for beta
204 oxidation, and a fatty acid desaturase (R4YV65/C34830; 4-fold higher spectral count) (enzymes that
205 incorporate double bonds into the hydrocarbon chains of fatty acids to yield unsaturated fatty acids
206 prior to activation for beta oxidation) and its associated oxidoreductase (R4YRU8/C34840; exclusively
207 expressed on *n*-C_{14}) (Fig 2).

208

209 **Cold induced proteins:** Of the 47 proteins with significantly higher spectral counts during growth at
210 4°C, 10 (21%) were identified by sequence homology to be involved in chemotaxis and motility
211 (Table S2; Fig 3A). Six methyl-accepting chemotaxis proteins (MCPs; R4YJH8/C01760;
212 R4YSY1/C11730; R4YQ71/ C12220, R4YT54/C25470, R4YV20/C32580, R4YRC3/C35950) which are
213 involved in signal transduction to flagella-associated proteins showed increased biosynthesis with
214 three to ten-fold greater spectral counts at 4°C compared to 16°C (Fig 3B). A methyltransferase,
215 CheR (R4YL24/C11900), which reversibly methylates the MCPs causing clockwise flagella rotation,
216 was exclusively detected at 4°C (Fig 3C). Methylesterase CheB proteins (R4YJA1; R4YL51; R4YL66)

217 coded by three genes present on the *O. antarctica* genome (C00950; C12250; C12450), which
218 reversibly demethylates the MCPs causing anticlockwise flagella rotation, were not detected.
219 Expression of two CheY proteins (R4YLC5/C12610 and R4YUQ1/C38770), which binds to components
220 of the flagella motor also causing clockwise flagella rotation, were 2.6-fold higher at 4°C (Fig 3C). An
221 acetyl-CoA synthetase (AcsA; R4YVD0/C38080) which acetylates the CheY proteins had 12-fold
222 greater expression at 4°C (Fig 3B). Flagellin (R4YSZ8/C12030) had 2.2-fold higher spectral counts at
223 4°C (Fig 3D) and based on functional family (FunFam) assignment in CATH the protein is the B
224 subunit, FlaB (Evalue-$9.4e^{-56}$). A transcriptional flagella regulator, FleQ (R4YT01/C12080) and the
225 protein FliL (R4YL55/C12300) which contributes to torque generation in flagella at higher motor
226 loads, also had 1.4-fold and 2.5-fold higher spectral counts respectively at 4°C (Fig 3D).

227 Other proteins with a significant increase in spectral counts at 4°C (Table S2) had roles in
228 proline metabolism, oxidative stress response, RNA metabolism, ribosome maturation and cold
229 tolerance. The spectral counts for the bifunctional protein PutA (R4YV58/C34480) were 26-fold higher
230 (Fig. 4). For the catalase-peroxidase KatG (R4YMH2/C17540) they were 2.5-fold higher. The RNA
231 helicase DeaD (R4YKT5/C10600) was 1.5-fold greater at 4°C and the ribosome assembly factor, RhlE
232 (R4YQ17/C00680) was 2-fold higher. Surprisingly, the spectral counts for cold-adapted chaperonin
233 Cpn60 (R4YPX4/C29610) were 1.5-fold less abundant at 4°C (Table S2).

234 **Discussion**

235 ***Growth on alkanes*****:** Previous studies have not shown the substrate range of *O. antarctica* with it
236 only being tested in single substrate microcosms enriched with the *n*-alkane tetradecane (*n*-C_{14})
237 (Yakimov et al., 2003; Kube et al., 2013). *O. antarctica* was unable to grow on long-chain alkanes
238 greater than 24 carbon atoms long and this was confirmed by growth tests (Fig S1). *O. antarctica*
239 may not be able to utilize long-chain alkanes as it lacks the genes which code for enzymes necessary
240 for degradation (e.g. *almA, ladA*) and the low water solubility of these compounds leads to reduced
241 bioavailability (Feng et al., 2007; Throne-Holst et al., 2007).

At low temperatures, the growth rate or the rate of substrate oxidation for hydrocarbon-degrading bacteria is generally observed to decrease, which is thought to be a result of reduced enzymatic activity rates (Bisht et al., 2015), but *O. antarctica* can maintain rapid growth. Eleven enzymes were cloned and characterised from *O. antarctica* and exhibited significant catalytic activity at 4°C but were not truly psychrophilic as they did not show poor activity at higher temperatures (Kube et al., 2013). In fact, the enzymes tested had their activity optima at temperatures significantly higher than those in the environment (20°-50°C). The genome of *O. antarctica* revealed it has acquired a large proportion of its genes, including some of those involved in hydrocarbon metabolism, through horizontal gene transfer (Kube et al., 2013). There is a possibility these genes were gained from other bacteria with different temperature preferences. Considering that waters in Polar regions hardly warm up above 4-6°C and the fact the proteins exhibit generally higher temperature optima this indicates some of the enzymes found in *O. antarctica* are functioning at a large range of temperatures which is sufficient to facilitate active growth of this bacterium if hydrocarbons become available. In addition, *O. antarctica* has been shown to contain chaperonins Cpn60 and Cpn10 that when expressed heterogeneously, can significantly decrease the growth temperature of a mesophilic host due to their hyperactivation at low temperatures (4-12°C) (Ferrer et al., 2003). Kube et al. (2013) suggests this chaperonin system may fine-tune central metabolism at low temperatures and indirectly alkane utilization. The origin of the hydrocarbon degradation genes from potentially more mesophilic hydrocarbon degraders, their versatile activity temperature range and the use of a cold-adapted chaperonin system may explain why there was no significant difference in the growth rates at 4 and 16°C. The growth rates calculated in this study were in a similar range to those for other OHCB growing on the same substrates, such as *Alcanivorax borkumensis* SK2 (Gregson et al., 2019) and *Thalassolituus oleivorans* MIL-1 (Gregson et al., 2018).

Alkane induced proteins: The first step in alkane degradation is the introduction of an oxygen atom to the terminal carbon of an alkane by an alkane monooxygenase producing a corresponding primary alcohol (e.g. tetradecane to 1-tetradecanol). The genome of *O. antarctica* has three genes for alkane monooxygenases (C23040; C34350; C34450) which based on a census of Gammaproteobacteria with sequenced genomes, is the largest amount along with *Marinobacter hydrocarbonoclasticus* VT8 (Márquez and Ventosa, 2005; Kube et al., 2013). Other hydrocarbonoclastic bacteria are known to express only one class of alkane oxidising enzymes (e.g. AlkB, CYP153, AlkW) (van Beilen et al., 2006; Lo Piccolo et al., 2011; Nie et al., 2014). However, they have multiple genes encoding different isozymes of the same enzyme which could enable the bacterium to have a broader substrate range and allow more efficient regulation of their metabolism. This may also be the case for *O. antarctica*.

The first alkane monooxygenase (R4YNV2/C23040) which is homologous to AlkB2 from *Alcanivorax dieselolei* B-5 (B5T_00103) and *Alcanivorax borkumensis* SK2 (ABO_0122), was not detected in our dataset. The expression of *alk* genes may be dependent on the bacterial growth phase with the expression of *alkB2* during the early exponential phase and *alkB1* in the mid to late exponential phase (Marin et al., 2003). As proteins were extracted in the mid-exponential phase this may explain why the AlkB2 homolog was not detected. In addition, it is possible that this gene would be expressed during growth on a different length hydrocarbon. There is plenty of evidence provided by Kube et al. (2013) that show this gene (C23040) was acquired through horizontal gene transfer (HGT). C23040 is located in the region between genomic island (GI) GI:19 and GI:20, which is rich in transposases indicating HGT. The presence of a prophage within the genome of *O. antarctica* suggests phage-mediated HGT has occurred and several genomic islands were also found to be homologous to the plasmid pCP301 from *Shigella* suggesting plasmid-mediated HGT. The second alkane monooxygenase (R4YQX3/C34350) was exclusively expressed on *n*-C_{14} whereas the third alkane monooxygenase (R4YQY4/C34450) was 12-fold greater on *n*-C_{14} compared to Tween indicating a small baseline constitutive expression with increased biosynthesis in response to alkane exposure. All three AlkB homologs have low sequence similarity to each other (<30%).

Upstream of both expressed alkane monooxygenases (C34350 and C34450) are open reading frames that code for proteins related to the AraC family of transcriptional regulators (C34330 and C34430) as seen in other *Alcanivorax* and *Pseudomonas* isolates. *alkB* regulation in Gram-negative bacteria mostly belong to the AraC or LuxR family (Ratajczak et al., 1998; van Beilen et al., 2001, Tani et al., 2001; van Beilen et al., 2004; Liu et al, 2011). Some of the regulators in Gram-negative bacteria can directly respond to *n*-alkanes and induce *alkB* gene expression (Marin et al., 2001; Tani et al., 2001). These regulators are divergently transcribed with *alkB* (Whyte et al., 2002). The low sequence similarity between the two AraC family regulators in *O. antarctica* (36%) may suggest distinct regulatory mechanisms for C34350 and C34450 expression by *n*-alkanes.

The genome also contains a P450 cytochrome (C17420) which was presumed to be involved in terminal hydroxylation of hydrocarbons (Kube et al., 2013). However, in all our treatments within this study, the cytochrome was not detected during growth, suggesting it is not involved in alkane degradation in *O. antarctica* and performs another function. This result is supported by previous work showing the CYP153 family of P450 oxygenases, which are known to be involved in alkane degradation, contain a well-conserved N-terminal (MFIAMDPP) and C-terminal (HTCMGNRL) which is absent from the cytochrome P450 in *O. antarctica* (Kubota et al., 2005; Wang et al., 2010).

The second and third step in alkane degradation is the conversion of the primary alcohol to its corresponding aldehyde catalysed by an alcohol dehydrogenase, followed by conversion of the aldehyde to its corresponding fatty acid by an aldehyde dehydrogenase. The alcohol dehydrogenase AlkJ (R4YRA7/C34360), which shows amino acid homology to AlkJ from *Alcanivorax borkumensis* SK2 (van Beilen et al., 1992). *O. antarctica* also expressed an oxidoreductase (R4YJ92/C00500) that is homologous to an alcohol dehydrogenase LaoA from *Pseudomonas aeruginosa* (PA0364; 58% identity). LaoA from *P. aeruginosa* is part of a gene cluster that was shown to oxidize the alcohols derived from the alkane degradation and also contains an inner membrane transport protein (LaoB/PA0365), an aldehyde dehydrogenase (LaoC/PA0366) and a transcriptional regulator

(LaoR/PA0367) (Panasia and Philipp, 2018). This genetic organisation is also seen in *O. antarctica* as the oxidoreductase (C00500) is part of a cluster consisting of genes coding for an inner membrane transport protein (C00510), an aldehyde dehydrogenase (C00520) and a TetR transcriptional regulator (C00530). Given that AlkJ (C34360) shows low similarity (31% identity) to LaoA (C00500) this means there are two distinct alcohol dehydrogenase mechanisms both active under alkane-degrading conditions in *O. antarctica*. In addition, we checked for this genetic organization (alcohol dehydrogenase, inner membrane transport protein, aldehyde dehydrogenase and transcriptional regulator grouped in an operon) in the genomes of other key marine obligate *n*-alkane-degrading bacteria and found the same organisation in *Alcanivorax borkumensis* SK2 (ABO_0085-ABO_0088; Schneiker et al., 2006), *Alcanivorax dieselolei* B5 (B5T_00037-B5T_00040; Lai et al., 2012), *Alcanivorax jadensis* T9A (T9A_01032-T9A_01035; Parks et al., 2017), *Thalassolituus oleivorans* MIL-1 (TOL_0221-TOL_0224; Golyshin et al., 2013), and *Marinobacter hydrocarbonoclasticus* SP17 (MARHY_3473-MARHY_3476; Grimaud et al., 2012). The increased protein biosynthesis of this system observed in our analysis of *O. antarctica* and observations in the genomes other OHCB, suggest this enzyme system is not just restricted to *P. aeruginosa* and may be much more widespread amongst other marine hydrocarbon-degrading bacteria. This may represent an additional/alternative oxidation system for the alcohols derived from alkane degradation compared to systems involving the well characterised dehydrogenase AlkJ, potentially enhancing the substrate range of these marine hydrocarbon-degrading bacteria.

***Cold induced proteins*:** As bacterial cells move through heterogenous environments, they encounter various fluids of different viscosities. Under changing conditions (e.g. temperature) bacteria experience different levels of viscous drag (or mechanical load) on their flagella. The physical properties of water are temperature-dependent, particularly viscosity. A change in temperature from 16 to 4°C is associated with an increase in kinematic viscosity from 1.0508×10^{-6} to 1.6262×10^{-6} $m^2 s^{-1}$ [1]. The evidence that *O. antarctica* is responding to a higher viscosity environment at 4°C was the increased biosynthesis of particular aspects of the flagellar that will generate sufficient force for

rotation including FleQ, FliL and FlaB. Flagella assembly is controlled by FleQ, an NtrC-like transcriptional regulator which controls synthesis of flagellar genes and its expression, in other flagellated bacteria, was shown to be cold induced, based on an 83% decrease in *fleQ* transcripts at 30°C compared to 4°C (Soutourina et al., 2001). The flagellar protein, FliL, which is a single-transmembrane protein with a large periplasmic region and associates with the flagellar basal body, has been found to be important for the function of the motor under high-load conditions, such as highly viscous environments, by recruiting or stabilizing the stators or by increasing their efficiency, leading to greater torque generation (Partridge et al., 2015; Takekawa et al., 2019). Flagellin is the major structural protein of the flagella filaments, which in *O. antarctica* is composed of the subunits FlaA and FlaB. It has been suggested that by altering the ratio of the flagellin subunits the shape of the filament may be optimally adapted to different environmental circumstances (e.g. greater density), with FlaB protein levels increasing at lower temperatures (Wösten et al., 2010). The relative amounts of the flagellin subunits could determine the degree of flexibility or stiffness of the flagellum, and the modulation of these amounts, with increased FlaB expression, adapts the organelle to changes in the viscosity experienced by *O. antarctica*.

The increased viscosity of fluids at lower temperatures will also influence the motility of bacteria travelling through them. *O. antarctica* has a monopolar, monotrichous flagellum meaning it lacks the "run-and-tumble" motility mechanism seen in the peritrichous *E. coli* (Kube et al., 2013). It most likely uses "run-and-reverse" swimming where the flagellum rotates counter-clockwise (CCW) to push the cell forward and clockwise (CW) to pull it backwards. This type of motility is very prevalent in the ocean being used in approximately 70% of marine isolates (Johansen et al., 2002). The main cause to increase the flagella switching frequency (CCW to CW) is the chemotaxis signalling pathway and several components of this pathway showed increased biosynthesis at 4°C. In the pathway stimulation of the chemotaxis receptors, also known as methyl-accepting chemotaxis proteins (MCPs), is followed by phosphorylation or acetylation of the response regulator CheY; phosphorylated (CheY-P); or acetylated (CheY-Asc); CheY then associates with the rotor of the flagella motor, and the motor

changes direction to CW (Porter et al., 2011; Takabe et al., 2017). Six MCPs showed increased biosynthesis (Fig 3B) and may be detecting changes in temperature (thermoreceptors), viscosity (viscoreceptors), or both, through their periplasmic domains. Following activation and signal transduction through these MCPs, *O. antarctica* needs to adapt to a background level of the attractant (i.e. temperature/viscosity) by resetting the receptor proteins to a non-signalling state. This is done by CheR, that was exclusively expressed at 4°C (Fig 3B), which methylates conserved glutamate residues in the cytoplasmic signalling domain of the MCPs. The response regulators, CheY, in *O. antarctica*, are most likely activated through acetylation rather than phosphorylation due to the 12-fold increased biosynthesis of acetyl-CoA synthetase (AcsA), which adds an acetyl group at conserved lysine residues (Barak and Eisenbach, 2001). This is also reinforced by the increased biosynthesis of CheZ which dephosphorylates CheY-P (Barak and Eisenbach, 2004). The increased biosynthesis of these proteins indicates a shift to CW flagellar rotation which would lead to more reversal events. *O. antarctica* may be a poor swimmer in low viscosity environments and this could be one of the reasons it is outcompeted in more temperate areas. The viscosity-induced increase in reversal events would limit cell migration, resulting in the accumulation of *O. antarctica* cells in an area where it can outcompete other bacteria. Alternatively, the cells could be more stressed at 16°C, as it is slightly outside the growth optima of *O. antarctica*, and are looking for a better environment (colder) to accumulate.

Low temperatures also increase the production of reactive oxygen species (ROS) due to the generation of heat accompanied by increased respiration and therefore oxygen consumption. ROS induce different forms of cell damage, disturb the redox state and can change the activity of several metabolic enzymes leading to oxidative stress (Blagojevic et al., 2011). Evidence to suggest *O. antarctica* is counteracting oxidative stress at lower temperatures was the increased biosynthesis of the proline utilisation protein, PutA, and the catalase-peroxidase, KatG. Previous studies have suggested that proline metabolism increases oxidative stress resistance (Zhang et al., 2015). PutA catalyses the oxidation of proline to glutamate and is made up of two domains, a proline

dehydrogenase (PRODH) domain, which couples the two electron oxidation of proline with the reduction of ubiquinone, and a delta-1-prroline-5-carboxylate dehydrogenase (P5CDH) domain, that converts a metabolic intermediate (P5C) into glutamate generating NADH (Menzel and Roth, 1981; Moxley et al., 2011). Proline metabolism will generate hydrogen peroxide (H_2O_2) through the PRODH domain with electrons going into the ubiquinone pool and the P5CDH domain produces NADH, both of which would lead to increased electron flux through the respiratory chain. Increases in the endogenous levels of H_2O_2 would then be enough to induce expression of proteins active against ROS e.g. KatG. Hydroperoxidase I (coded by *katG*) expression is induced by H_2O_2 and when expressed is active against ROS (Zhang et al., 2015). This indicates proline metabolism via PutA may offer *O. antarctica* a competitive advantage over other bacteria in harsh oxidative/low temperature environments through a preadaptive effect involving greater endogenous H_2O_2 production and enhanced peroxidase expression.

O. antarctica has previously been shown to express cold-adapted chaperonins Cpn60 (C29610) and Cpn10 (C29620) which are homologous to the *E. coli* GroELS system, promoting the folding and assembly of over 30% of *E. coli*'s cellular proteins (Gething and Sambrook, 1992; Ferrer et al., 2003; Kube et al., 2013). GroELS rapidly loses its refolding activity at temperatures below 37°C but Cpn60/Cpn10 functions well at low temperatures (Ferrer et al., 2003). Coexpression of Cpn60/Cpn10 from *O. antarctica* in *E. coli*, lowered its minimal growth temperature below 15°C (Ferrer *et al.*, 2003, 2004). These findings indicated the chaperonins play a key role in cold sensitivity, adaption or tolerance. However, Cpn60 was abundantly detected at both the warmer 16°C and colder 4°C temperature, suggesting these chaperonins are required for protein folding at all temperatures (Table S2). *O. antarctica* also has a GroELS chaperonin system coded by its genome. The biosynthesis of GroEL (C29610) chaperonin was 1.6-fold higher at 16°C and the GroES (C29620) chaperonin was not detected at either temperature, indicating this system is induced by and folds protein at higher temperatures.

Conclusion: This study contributes to our understanding of a key psychrophilic hydrocarbon-degrading bacteria that dominates microbial communities in cold marine environments following oil spills. It has demonstrated *O. antarctica* has a very restricted substrate range, even compared to other OHCB, and might explain why it is outcompeted in warmer oil-contaminated marine environments by more metabolically versatile hydrocarbon-degraders. The study also identified key hydrocarbon-degrading enzymes relating their expression to the physiological activity of *O. antarctica* and validated previous functional genomic expression analysis performed in Kube et al., (2013) that putatively assigned genes to alkane degradation pathways. This study also highlights potential mechanisms *O. antarctica* utilises that may provide it with ecological competitiveness at low temperatures. These include structural changes in the flagella to generate sufficient force to counteract increased viscosity, use of chemotaxis machinery to alter flagella rotation causing accumulation of cells in beneficial areas, and increased proline metabolism to generate H_2O_2 enhancing hydroperoxidase expression to counteract oxidative stress. Overall, we have a much deeper insight into the life of an obligate hydrocarbonoclastic bacteria in the cold but whether these metabolic pathways and adaptation mechanisms exist in other marine hydrocarbon-degrading psychrophiles requires further investigation.

Experimental procedures

Culture conditions and growth of *O. antarctica* RB-8: Cultures of *Oleispira antartica* RB-8 (DSM 14852) were established in sterile 100ml culture flasks containing 50ml of ONR7a media (Dyksterhouse et al, 1995).Triplicate cultures were established for each temperature and time point to be sampled that were enriched separately with the following alkanes at a final concentration of 0.1% w/v: decane (C_{10}), dodecane (C_{12}), hexadecane (C_{16}), eicosane (C_{20}), tetracosane (C_{24}), octacosane (C_{28}), and dotriacontane (C_{32}) and the branched alkane pristine (Sigma-Aldrich). Non-hydrocarbon controls cultures were established with Tween 80 (polyethylene glycol sorbitan monooleate) at 1% v/v. Tween 80 was chosen to be the non-hydrocarbon control as OHCB exhibit a 'BIOLOG anomaly' i.e, growth

445 occurs on only 2 of the 95 organic growth substrates in the BIOLOG1 system, namely Tween 40 and
446 Tween 80, substrates that contain long-chain alkyl moieties. No-carbon controls (ONR7a media with
447 no added carbon source) were also established along with uninoculated cultures to determine
448 whether any hydrocarbon losses were abiotic. The cultures were incubated at 4 and 16°C, at 60rpm,
449 for 21 days. Growth curves were determined from increase in optical density over time at 600nm on
450 a NanoDrop 1000 Spectrophotometer.

451 **GC-MS analysis:** Alkanes were extracted in 5ml of hexane or hexane:dichloromethane (1:1) for C_{32}.
452 The vials were shaken vigorously. Samples were then centrifuged (4600 × g, 15 mins). 1 ml of the upper
453 solvent phase was taken and diluted with hexane to an appropriate concentration for GC-MS analysis.
454 Deuterated nonadecane (C_{19}^{d40}) was added as an internal standard at 5µg ml^{-1}. Alkanes were identified
455 and quantified using a TRACE Ultra Gas Chromatograph (ThermoFisher Scientific) coupled with a
456 TRACE DSQ Mass Spectrometer (ThermoFisher Scientific) operated at 70eV in positive ion mode.
457 Chromatography was performed by splitless injection with helium as the carrier gas, onto a 30m ×
458 0.25mm × 0.25mm fused silica capillary column Rtx-5MS (Restek) (0.25µm film thickness). The injector
459 temperature was 300°C, and the oven program was 65°C for 2 min, increasing to 310°C at 20°C min^{-1}
460 then held for 18 mins. External multi-level calibrations were performed using an alkane standard mix
461 (C_8-C_{40}) (Sigma-Aldrich) with quantification of five levels ranging from 0.250-16 ng μl^{-1}. The mass
462 spectrometer was operated in full scan mode (range *m/z* 50-650), with identification of target analytes
463 based on retention times of the analytical standards and mass spectrum (intensity vs. mz).
464 Quantification was performed by integrating the peak of target analytes at specific *m/z* ratios.

465 ***Proteomic analysis*:** Cultures of *Oleispira antarctica* RB-8 (DSM No: 14852, Type strain) were grown in
466 160 ml culture flasks containing 50 ml of ONR7a artificial seawater media (Dyksterhouse et al, 1995
467 supplemented with either *n*-tetradecane (*n*-C_{14}) (Sigma-Aldrich) or the non-hydrocarbon control
468 Tween 80 (0.1% v/v) as the sole carbon source and incubated at either 4°C or 16°C (*n*=3). Cells were
469 harvested for protein extraction after 4 days in mid-exponential phase by centrifugation (4600 × g, 15

mins). The cell pellet was washed in 2ml of Dulbecco's Phosphate-Buffered Saline (Sigma-Aldrich) centrifuged (10,500 × g, 5 mins). Total proteins was extracted by resuspending the cell pellet in 50µl of protein extraction buffer (62.5mM TRIS, 10% glycerol w/v, 12mM dithiothreitol (DTT), 2% sodium dodecyl sulfate (SDS) v/v and 1 Pierce Protease Inhibitor Tablet per 50 ml) and heating in a water bath (95°C, 12 mins) fully lysing the cells, and then centrifuged (10,500 × g, 5 mins) to remove cell debris. Proteins extracts were visualised by SDS-PAGE before performing in-gel digestion with trypsin and subsequent analysis of the peptides on a hybrid high-resolution LTQ/Orbitrap Velos LC-MS/MS instrument (Thermo Scientific) as previously described (McKew et al, 2013)

***MS/MS analysis*:** MS/MS analysis was performed using the methods previously used in Gregson et al., 2018. Uniprot protein sequences from the *O. antarctica* RB-8 genome (Kube et al., 2013) were used to perform identification. Proteins were validated using the default settings in MaxQuant and Andromeda with a minimum of at least one peptide, but that any such protein had to be unambiguously identified by peptides that were unique to that protein. Spectral counts were normalised using the Total Spectral Count (TSpC) method (Dong et al., 2007) where the sample with the highest number of TSpC is chosen and the remaining samples are normalised to it to account for small differences in total detected spectral counts per run.. The Normalized Spectral Abundance Factor (number of spectral counts divided by the length of the polypeptide, expressed as percentage for each protein compared to the sum of this ratio for all the detected proteins) was also calculated as longer proteins are expected to produce more peptides (Florens et al., 2006; Zybailov et al., 2006).

***Statistical analysis*:** Differential expression analysis was performed on normalized spectral count data in the OMICS package of XLSTAT-Premium Version 2016.1 (Addinsoft) to identify differentially expressed proteins by analysis of variance (ANOVA) with Tukey Honestly Significant Difference post-hoc test for pairwise comparisons, according to the factors 'substrate' (two levels: *n*-C_{14}, Tween 80) and 'temperature' (two levels: 4°C or 16°C). The Benjamini-Hochberg False Discovery Rate corrections procedure was used for post-hoc p-value corrections (Benjamini and Hochberg, 1995).

Bioinformatic analysis: All proteins showing a significant (P<0.05) increase in spectral count on hydrocarbons were subjected to a BLASTp (Basic Local Alignment Search Tool) (Altschul et al, 1990) homology search where the protein was compared to the nr database (non-redundant sequences from GenBank CDS translations, PDB, Swiss-Prot, PIR and PRF). Protein family and domain analysis was carried out in Pfam v30.0 (Finn et al, 2016). SCOOP (Simple Comparison of Outputs Program) (Bateman and Finn, 2007) was used to detect relationships between families in the Pfam database. Proteins were assigned to functional families by hierarchical classification of protein domains based on their folding patterns in CATH v4.1 (Class, Architecture, Topology, Homology) (Sillitoe et al, 2015). Full length secondary and tertiary structure predictions, functional annotations on ligand-binding sites, enzyme commissions numbers and gene ontology terms were generated using the I-TASSER SERVER (Zhang, 2008).

Acknowledgements

This research was supported by the Eastern Academic Research Consortium (Eastern ARC) and the Natural Environment Research Council (NE/R016569/1). We acknowledge the funding from the European Commission of the Horizon 2020 project "INMARE" (Contract Nr 634486)

Table and Figure Legends

Figure 1 – (A) Principle component analysis of replicate *O. antarctica* RB-8 proteomes during growth on tetradecane (*n*-C_{14}) and the non-hydrocarbon control Tween 80 (Tween) at 4°C and 16°C based on normalised spectral counts for proteins. (B) Violin plots of normalised LC-MS/MS spectral counts showing the distribution of detected proteins in *O. antarctica* RB-8 during growth on different substrates; *n*-C_{14} versus Tween (left; *n*-C14:Tween); and different temperature; 4°C versus 16°C (right; 4°C: 16°C). (C and D) Volcano plots of normalised LC-MS/MS spectral counts comparing *O. antarctica* RB-8 protein abundance during growth on different substrates; *n*-C_{14} versus Tween (left; *n*-C_{14}: Tween) and different temperatures; 4°C versus 16°C (right; 4°C:16°C). Larger data points (light and dark grey) represent differentially expressed proteins with *P*-values below 0.05.

Figure 2 – (A) Normalized Spectral counts (means ±SE; *n*=3) of differentially expressed alkane degradation proteins during growth on the *n*-alkane tetradecane (*n*-C_{14}; light grey and dark grey), the non-hydrocarbon control (Tween 80; white and black) at 4° and 16°C in *Oleispira antarctica* RB-8. (B) The monooxygenase (AlkB; C34350/C34450) introduces oxygen into the *n*-alkane converting it into a primary alcohol. This alcohol is further oxidized to an aldehyde and then a fatty acid by the alcohol dehydrogenase (ADH; C00500/C34360) and aldehyde dehydrogenase (ALDH; C00520/C11600), respectively. The fatty acid desaturase (FAD; C34830) incorporates double bonds into the hydrocarbon chain of the saturated fatty acid to yield unsaturated fatty acids. The fatty acid-CoA ligase (FA-CoAL; C09310) catalyses the conversion of unsaturated or saturated fatty acids to their active form acyl-CoAs for degradation via β-oxidation.

Figure 3 – (A) Schematic diagram demonstrating the putative roles of proteins with significantly higher spectral counts involved in chemotaxis and motility in *Oleispira antarctica* RB-8 during growth at 4°C. (B-D) Normalized Spectral counts (means ±SE; *n*=6) for the chemotaxis proteins during growth at 4°C (white) compared to 16°C (grey) in *Oleispira antarctica* RB-8 are presented and separated based on their cellular location. B – Inner membrane; C – Cytoplasmic; D – Outer membrane.

Figure 4- (A) Normalized Spectral counts (means ±SE; *n*=6) for the proline utilisation A (PutA) flavoenzyme (R4YV58/C34480) and the catalase-peroxidase KatG (R4YMH2/C17540) with increased biosynthesis during growth at 4°C (white) compared to 16°C (grey) in *Oleispira* RB-8. (B) The proline utilisation A (PutA) flavoenzyme consists of a proline dehydrogenase (PRODH) and a Δ1-pyrroline-5-carboxylate dehydrogenase (P5CDH) domains. The PRODH domain contains a flavin adenine dinucleotide (FAD) cofactor and couples the oxidation of proline (Pro) to Δ1-pyrroline-5-carboxylate (P5C) with the reduction of ubiquinone (CoQ). P5C is then hydrolysed to glutamate-γ-semialdehyde (GSA) which is oxidised to glutamate (Glu) by the NAD+ dependent P5CDH domain. Molecular oxygen (O_2) is reduced by the influx of electrons from electron donors (CoQH2 and NADH) which

546 leads to the formation of superoxide ($^{\bullet}O_2$). This superoxide is then converted to hydrogen peroxide
547 (H_2O_2) either non-enzymatically or enzymatically by superoxide dismutase. H_2O_2 then induces the
548 biosynthesis of the catalase-peroxidase, KatG, which is active against reactive oxygen species (ROS).

549
550

551 **References**

552 Altschul, S.F., Gish, W., Miller, W., Myers, E.W., and Lipman, D.J. (1990) Basic local alignment search
553 tool. *J. Mol. Biol.* **215**: 403–410.

554 and, T.B., Ferlenghi‡, I., and, I.I., and Dreyfus, M. (2004) Studies on Three *E. coli* DEAD-Box Helicases
555 Point to an Unwinding Mechanism Different from that of Model DNA Helicases†.

556 Ando, Y. and Nakamura, K. (2006) *Bacillus subtilis* DEAD protein YdbR possesses ATPase, RNA
557 binding, and RNA unwinding activities. *Biosci. Biotechnol. Biochem.* **70**: 1606–15.

558 Armbruster, C.E., Hodges, S.A., Smith, S.N., Alteri, C.J., and Mobley, H.L.T. (2014) Arginine promotes
559 *Proteus mirabilis* motility and fitness by contributing to conservation of the proton gradient
560 and proton motive force. *Microbiologyopen* **3**: 630–641.

561 Arora, S.K., Ritchings, B.W., Almira, E.C., Lory, S., and Ramphal, R. (1997) A transcriptional activator,
562 FleQ, regulates mucin adhesion and flagellar gene expression in *Pseudomonas aeruginosa* in a
563 cascade manner. *J. Bacteriol.* **179**: 5574–81.

564 Auman, A.J., Breezee, J.L., Gosink, J.J., Kämpfer, P., and Staley, J.T. (2006) *Psychromonas ingrahamii*
565 sp. nov., a novel gas vacuolate, psychrophilic bacterium isolated from Arctic polar sea ice. *Int. J.*
566 *Syst. Evol. Microbiol.* **56**: 1001–1007.

567 Baker, A.E. and O'Toole, G.A. (2017) Bacteria, Rev Your Engines: Stator Dynamics Regulate Flagellar
568 Motility. *J. Bacteriol.* **199**: JB.00088-17.

569 Baker, M.D., Wolanin, P.M., and Stock, J.B. (2006) Signal transduction in bacterial chemotaxis.
570 *BioEssays* **28**: 9–22.

571 Barak, R. and Eisenbach, M. (2001) Acetylation of the response regulator, CheY, is involved in
572 bacterial chemotaxis. *Mol. Microbiol.* **40**: 731–43.

573 Barak, R. and Eisenbach, M. (2004) Co-regulation of Acetylation and Phosphorylation of CheY, A
574 Response Regulator in Chemotaxis of Escherichia coli. *J. Mol. Biol.* **342**: 375–381.

575 Barak, R., Prasad, K., Shainskaya, A., Wolfe, A.J., and Eisenbach, M. (2004) Acetylation of the
576 Chemotaxis Response Regulator CheY by Acetyl-CoA Synthetase Purified from *Escherichia coli*.
577 *J. Mol. Biol.* **342**: 383–401.

578 Barak, R., Welch, M., Yanovsky, A., Oosawa, K., and Eisenbach, M. (1992) Acetyladenylate or its
579 derivative acetylates the chemotaxis protein CheY in vitro and increases its activity at the
580 flagellar switch. *Biochemistry* **31**: 10099–10107.

581 Bateman, A. and Finn, R.D. (2007) SCOOP: a simple method for identification of novel protein
582 superfamily relationships. *Bioinformatics* **23**: 809–814.

583 van Beilen, J.B., Funhoff, E.G., van Loon, A., Just, A., Kaysser, L., Bouza, M., et al. (2006) Cytochrome
584 P450 alkane hydroxylases of the CYP153 family are common in alkane-degrading eubacteria
585 lacking integral membrane alkane hydroxylases. *Appl. Environ. Microbiol.* **72**: 59–65.

586 van Beilen, J.B., Marin, M.M., Smits, T.H.M., Rothlisberger, M., Franchini, A.G., Witholt, B., and Rojo,
587 F. (2004) Characterization of two alkane hydroxylase genes from the marine
588 hydrocarbonoclastic bacterium *Alcanivorax borkumensis*. *Environ. Microbiol.* **6**: 264–273.

589 van Beilen, J.B., Panke, S., Lucchini, S., Franchini, A.G., Röthlisberger, M., and Witholt, B. (2001)
590 Analysis of *Pseudomonas putida* alkane-degradation gene clusters and flanking insertion
591 sequences: evolution and regulation of the alk genes. *Microbiology* **147**: 1621–30.

592 van Beilen, J.B., Penninga, D., and Witholt, B. (1992) Topology of the membrane-bound alkane
593 hydroxylase of *Pseudomonas oleovorans*. *J. Biol. Chem.* **267**: 9194–201.

594 Benjamini, Y. and Hochberg, Y. (1995) Controlling the False Discovery Rate: A Practical and Powerful
595 Approach to Multiple Testing. *J. R. Stat. Soc. Ser. B* **57**: 289–300.

596 Berney, M. and Cook, G.M. (2010) Unique Flexibility in Energy Metabolism Allows *Mycobacteria* to
597 Combat Starvation and Hypoxia. *PLoS One* **5**: e8614.

598 Bissett, A., Bowman, J., and Burke, C. (2006) Bacterial diversity in organically-enriched fish farm
599 sediments. *FEMS Microbiol. Ecol.* **55**: 48–56.

600 Blagojevic, D.P., Grubor-Lajsic, G.N., and Spasic, M.B. (2011) Cold defence responses: the role of
601 oxidative stress. *Front. Biosci. (Schol. Ed).* **3**: 416–27.
602

603 Blat, Y. and Eisenbach, M. (1996) Oligomerization of the phosphatase CheZ upon interaction with the
604 phosphorylated form of CheY. The signal protein of bacterial chemotaxis. *J. Biol. Chem.* **271**:
605 1226–31.

606 Brakstad, O.G. and Bonaunet, K. (2006) Biodegradation of Petroleum Hydrocarbons in Seawater at
607 Low Temperatures (0–5 °C) and Bacterial Communities Associated with Degradation.
608 *Biodegradation* **17**: 71–82.

609 Brakstad, O.G., Nonstad, I., Faksness, L.-G., and Brandvik, P.J. (2008) Responses of microbial
610 communities in Arctic sea ice after contamination by crude petroleum oil. *Microb. Ecol.* **55**:
611 540–52.

612 Bren, A. and Eisenbach, M. (2000) How signals are heard during bacterial chemotaxis: protein-
613 protein interactions in sensory signal propagation. *J. Bacteriol.* **182**: 6865–73.

614 Bren, A., Welch, M., Blat, Y., and Eisenbach, M. (1996) Signal termination in bacterial chemotaxis:

615 CheZ mediates dephosphorylation of free rather than switch-bound CheY. *Proc. Natl. Acad. Sci.*
616 *U. S. A.* **93**: 10090–3.

617 Cartier, G., Lorieux, F., Allemand, F., Dreyfus, M., and Bizebard, T. (2010) Cold Adaptation in DEAD-
618 Box Proteins. *Biochemistry* **49**: 2636–2646.
619

620 Cavener, D.R. (1992) GMC oxidoreductases. A newly defined family of homologous proteins with
621 diverse catalytic activities. *J. Mol. Biol.* **223**: 811–4.

622 Charollais, J., Dreyfus, M., and Iost, I. (2004) CsdA, a cold-shock RNA helicase from *Escherichia coli*, is
623 involved in the biogenesis of 50S ribosomal subunit. *Nucleic Acids Res.* **32**: 2751–2759.

624 Coulon, F., McKew, B.A., Osborn, A.M., McGenity, T.J., and Timmis, K.N. (2007) Effects of
625 temperature and biostimulation on oil-degrading microbial communities in temperate
626 estuarine waters. *Environ. Microbiol.* **9**: 177–186.

627 Curtis, J., Shearer, G., and Kohl, D.H. (2004) Bacteroid proline catabolism affects N(2) fixation rate of
628 drought-stressed soybeans. *Plant Physiol.* **136**: 3313–8.

629 Dasgupta, N., Ferrell, E.P., Kanack, K.J., West, S.E.H., and Ramphal, R. (2002) fleQ, the gene encoding
630 the major flagellar regulator of *Pseudomonas aeruginosa*, is sigma70 dependent and is
631 downregulated by Vfr, a homolog of *Escherichia coli* cyclic AMP receptor protein. *J. Bacteriol.*
632 **184**: 5240–50.

633 Dasgupta, N., Wolfgang, M.C., Goodman, A.L., Arora, S.K., Jyot, J., Lory, S., and Ramphal, R. (2003) A
634 four-tiered transcriptional regulatory circuit controls flagellar biogenesis in *Pseudomonas*
635 *aeruginosa*. *Mol. Microbiol.* **50**: 809–24.

636 DeLong, E.F., Preston, C.M., Mincer, T., Rich, V., Hallam, S.J., Frigaard, N.-U., et al. (2006) Community
637 Genomics Among Stratified Microbial Assemblages in the Ocean's Interior. *Science (80-.).* **311**:
638 496–503.

639 Derr, P., Boder, E., and Goulian, M. (2006) Changing the specificity of a bacterial chemoreceptor. *J.*
640 *Mol. Biol.* **355**: 923–932.

641 van Dillewijn, P., Soto, M.J., Villadas, P.J., and Toro, N. (2001) Construction and environmental
642 release of a *Sinorhizobium meliloti* strain genetically modified to be more competitive for
643 alfalfa nodulation. *Appl. Environ. Microbiol.* **67**: 3860–5.

644 Djordjevic, S. and Stock, A.M. (1998) Chemotaxis receptor recognition by protein methyltransferase
645 CheR. *Nat. Struct. Biol.* **5**: 446–450.

646 Dong, M.-Q., Venable, J.D., Au, N., Xu, T., Park, S.K., Cociorva, D., et al. (2007) Quantitative Mass
647 Spectrometry Identifies Insulin Signaling Targets in C. elegans. *Science (80-.).* **317**: 660–663.

648 Dong, C., Bai, X., Sheng, H., Jiao, L., Zhou, H., and Shao, Z. (2015) Distribution of PAHs and the PAH-
649 degrading bacteria in the deep-sea sediments of the high-latitude Arctic Ocean. *Biogeosciences*
650 **12**: 2163–2177.

651 Dons, L., Rasmussen, O.F., and Olsen, J.E. (1992) Cloning and characterization of a gene encoding
652 flagellin of *Listeria monocytogenes*. *Mol. Microbiol.* **6**: 2919–29.

653 Dyksterhouse, S.E., Gray, J.P., Herwig, R.P., Lara, J.C., and Staley, J.T. (1995) *Cycloclasticus pugetii*
654 gen. nov., sp. nov., an aromatic hydrocarbon-degrading bacterium from marine sediments. *Int.*
655 *J. Syst. Bacteriol.* **45**: 116–23.

656 Feller, G. and Gerday, C. (2003) Psychrophilic enzymes: hot topics in cold adaptation. *Nat. Rev.*
657 *Microbiol.* **1**: 200–208.

658 Feng, L., Wang, W., Cheng, J., Ren, Y., Zhao, G., Gao, C., et al. (2007) Genome and proteome of long-
659 chain alkane degrading *Geobacillus thermodenitrificans* NG80-2 isolated from a deep-
660 subsurface oil reservoir. Proc. Natl. Acad. Sci. 104: 5602–5607.

661 Ferrer, M., Chernikova, T.N., Timmis, K.N., and Golyshin, P.N. (2004) Expression of a temperature-

662 sensitive esterase in a novel chaperone-based *Escherichia coli* strain. *Appl. Environ. Microbiol.*
663 **70**: 4499–504.

664 Ferrer, M., Chernikova, T.N., Yakimov, M.M., Golyshin, P.N., and Timmis, K.N. (2003) Chaperonins
665 govern growth of *Escherichia coli* at low temperatures. *Nat. Biotechnol.* **21**: 1266–7.

666 Finn, R.D., Coggill, P., Eberhardt, R.Y., Eddy, S.R., Mistry, J., Mitchell, A.L., et al. (2016) The Pfam
667 protein families database: towards a more sustainable future. *Nucleic Acids Res.* **44**: D279–
668 D285.

669 Florens, L., Carozza, M.J., Swanson, S.K., Fournier, M., Coleman, M.K., Workman, J.L., and Washburn,
670 M.P. (2006) Analyzing chromatin remodeling complexes using shotgun proteomics and
671 normalized spectral abundance factors. *Methods* **40**: 303–11.

672 Fraiberg, M., Afanzar, O., Cassidy, C.K., Gabashvili, A., Schulten, K., Levin, Y., and Eisenbach, M.
673 (2015) CheY's acetylation sites responsible for generating clockwise flagellar rotation in
674 *Escherichia coli*. *Mol. Microbiol.* **95**: 231–44.

675 Gallegos, M.T., Schleif, R., Bairoch, A., Hofmann, K., and Ramos, J.L. (1997) Arac/XylS family of
676 transcriptional regulators. *Microbiol. Mol. Biol. Rev.* **61**: 393–410.

677 Gao, H., Yang, Z.K., Wu, L., Thompson, D.K., and Zhou, J. (2006) Global Transcriptome Analysis of the
678 Cold Shock Response of *Shewanellaoneidensis* MR-1 and Mutational Analysis of Its Classical
679 Cold Shock Proteins. *J. Bacteriol.* **188**: 4560–4569.

680 Gerdes, B., Brinkmeyer, R., Dieckmann, G., and Helmke, E. (2005) Influence of crude oil on changes
681 of bacterial communities in Arctic sea-ice. *FEMS Microbiol. Ecol.* **53**: 129–139.

682 Gertler, C., Näther, D.J., Cappello, S., Gerdts, G., Quilliam, R.S., Yakimov, M.M., and Golyshin, P.N.
683 (2012) Composition and dynamics of biostimulated indigenous oil-degrading microbial
684 consortia from the Irish, North and Mediterranean Seas: a mesocosm study. *FEMS Microbiol.*
685 *Ecol.* **81**: 520–536.

686 Gething, M.-J. and Sambrook, J. (1992) Protein folding in the cell. *Nature* **355**: 33–45.

687 Ghobakhlou, A.-F., Johnston, A., Harris, L., Antoun, H., and Laberge, S. (2015) Microarray
688 transcriptional profiling of Arctic *Mesorhizobium* strain N33 at low temperature provides
689 insights into cold adaption strategies. *BMC Genomics* **16**: 383.

690 Golyshin, P.N., Werner, J., Chernikova, T.N., Tran, H., Ferrer, M., Yakimov, M.M., et al. (2013)
691 Genome Sequence of *Thalassolituus oleivorans* MIL-1 (DSM 14913T). *Genome Announc.* **1**:
692 e0014113.

693 Gonzalez-Pedrajo, B., Minamino, T., Kihara, M., and Namba, K. (2006) Interactions between C ring
694 proteins and export apparatus components: a possible mechanism for facilitating type III
695 protein export. *Mol. Microbiol.* **60**: 984–998.

696 Grady, S.L., Malfatti, S.A., Gunasekera, T.S., Dalley, B.K., Lyman, M.G., Striebich, R.C., et al. (2017) A
697 comprehensive multi-omics approach uncovers adaptations for growth and survival of
698 *Pseudomonas aeruginosa* on *n*-alkanes. *BMC Genomics* **18**: 334.

699 Gregson, B.H., Metodieva, G., Metodiev, M. V, Golyshin, P.N., and McKew, B.A. (2018) Differential
700 Protein Expression During Growth on Medium Versus Long-Chain Alkanes in the Obligate
701 Marine Hydrocarbon-Degrading Bacterium *Thalassolituus oleivorans* MIL-1. *Front. Microbiol.* **9**:
702 3130.

703 Grimaud, R., Ghiglione, J.-F., Cagnon, C., Lauga, B., Vaysse, P.-J., Rodriguez-Blanco, A., et al. (2012)
704 Genome sequence of the marine bacterium *Marinobacter hydrocarbonoclasticus* SP17, which
705 forms biofilms on hydrophobic organic compounds. *J. Bacteriol.* **194**: 3539–40.

706 Gunasekera, T.S., Striebich, R.C., Mueller, S.S., Strobel, E.M., and Ruiz, O.N. (2013) Transcriptional
707 Profiling Suggests that Multiple Metabolic Adaptations are Required for Effective Proliferation
708 of *Pseudomonas aeruginosa* in Jet Fuel. *Environ. Sci. Technol.* **47**: 13449–13458.

709 Hara, A., Baik, S., Syutsubo, K., Misawa, N., Smits, T.H.M., van Beilen, J.B., and Harayama, S. (2004)

Cloning and functional analysis of alkB genes in *Alcanivorax borkumensis* SK2. *Environ. Microbiol.* **6**: 191–7.

Harayama, S., Kasai, Y., and Hara, A. (2004) Microbial communities in oil-contaminated seawater. *Curr. Opin. Biotechnol.* **15**: 205–214.

Harayama, S., Kishira, H., Kasai, Y., and Shutsubo, K. (1999) Petroleum biodegradation in marine environments. *J. Mol. Microbiol. Biotechnol.* **1**: 63–70.

Hazen, T.C., Dubinsky, E.A., DeSantis, T.Z., Andersen, G.L., Piceno, Y.M., Singh, N., et al. (2010) Deep-sea oil plume enriches indigenous oil-degrading bacteria. *Science* **330**: 204–8.

Herschlag, D. (1995) RNA chaperones and the RNA folding problem. *J. Biol. Chem.* **270**: 20871–4.

Jain, C. (2008) The *E. coli* RhlE RNA helicase regulates the function of related RNA helicases during ribosome assembly. *RNA* **14**: 381–9.

Johnson, T.L., Abendroth, J., Hol, W.G.J., and Sandkvist, M. (2006) Type II secretion: from structure to function. *FEMS Microbiol. Lett.* **255**: 175–186.

Jones, P.G., Mitta, M., Kim, Y., Jiang, W., and Inouye, M. (1996) Cold shock induces a major ribosomal-associated protein that unwinds double-stranded RNA in *Escherichia coli*. *Proc. Natl. Acad. Sci. U. S. A.* **93**: 76–80.

Jyot, J., Sonawane, A., Wu, W., and Ramphal, R. (2007) Genetic mechanisms involved in the repression of flagellar assembly by *Pseudomonas aeruginosa* in human mucus. *Mol. Microbiol.* **63**: 1026–1038.

Kasai, Y., Kishira, H., Sasaki, T., Syutsubo, K., Watanabe, K., and Harayama, S. (2002) Predominant growth of *Alcanivorax* strains in oil-contaminated and nutrient-supplemented sea water. *Environ. Microbiol.* **4**: 141–7.

733 Kathariou, S., Kanenaka, R., Allen, R.D., Fok, A.K., and Mizumoto, C. (1995) Repression of motility and
734 flagellin production at 37 degrees C is stronger in *Listeria monocytogenes* than in the
735 nonpathogenic species Listeria innocua. *Can. J. Microbiol.* **41**: 572–7.

736 Kimes, N.E., Grim, C.J., Johnson, W.R., Hasan, N.A., Tall, B.D., Kothary, M.H., et al. (2012)
737 Temperature regulation of virulence factors in the pathogen *Vibrio coralliilyticus*. *ISME J.* **6**:
738 835–846.

739 Kirby, M.F., Brant, J., Moore, J., Lincoln, S. (2018) PREMIAM - Pollution Response in Emergencies -
740 Marine Impact Assessment and Monitoring: Post-incident monitoring guidelines. Second
741 Edition. Science Series Technical Report. Cefad, Lowestoft, 176 pp
742 https://www.cefas.co.uk/premiam/guidelines/

743 Kohl, D.H., Straub, P.F., and Shearer, G. (1994) Does proline play a special role in bacteroid
744 metabolism? *Plant, Cell Environ.* **17**: 1257–1262.

745 Kostka, J.E., Prakash, O., Overholt, W.A., Green, S.J., Freyer, G., Canion, A., et al. (2011) Hydrocarbon-
746 degrading bacteria and the bacterial community response in gulf of Mexico beach sands
747 impacted by the deepwater horizon oil spill. *Appl. Environ. Microbiol.* **77**: 7962–74.

748 Kube, M., Chernikova, T.N., Al-Ramahi, Y., Beloqui, A., Lopez-Cortez, N., Guazzaroni, M.-E., et al.
749 (2013) Genome sequence and functional genomic analysis of the oil-degrading bacterium
750 *Oleispira antarctica*. *Nat. Commun.* **4**: 2156.

751 Kubota, M., Nodate, M., Yasumoto-Hirose, M., Uchiyama, T., Kagami, O., Shizuri, Y., and Misawa, N.
752 Isolation and Functional Analysis of Cytochrome P450 CYP153A Genes from Various
753 Environments.

754 Lai, Q., Li, W., and Shao, Z. (2012) Complete Genome Sequence of *Alcanivorax dieselolei* Type Strain
755 B5. *J. Bacteriol.* **194**: 6674–6674.

756 Larson, J.D., Jenkins, J.L., Schuermann, J.P., Zhou, Y., Becker, D.F., and Tanner, J.J. (2006) Crystal

757 structures of the DNA-binding domain of *Escherichia coli* proline utilization A flavoprotein and
758 analysis of the role of Lys9 in DNA recognition. *Protein Sci.* **15**: 2630–41.

759 Lee, Y.-H., Nadaraia, S., Gu, D., Becker, D.F., and Tanner, J.J. (2003) Structure of the proline
760 dehydrogenase domain of the multifunctional PutA flavoprotein. *Nat. Struct. Biol.* **10**: 109–114.

761 Lee, Y.-Y. and Belas, R. (2015) Loss of FliL alters Proteus mirabilis surface sensing and temperature-
762 dependent swarming. *J. Bacteriol.* **197**: 159–73.

763 Lele, P.P., Hosu, B.G., and Berg, H.C. (2013) Dynamics of mechanosensing in the bacterial flagellar
764 motor. *Proc. Natl. Acad. Sci.* **110**: 11839–11844.

765 Li, R., Chen, P., Gu, J., and Deng, J.-Y. (2013) Acetylation reduces the ability of CheY to undergo
766 autophosphorylation. *FEMS Microbiol. Lett.* **347**: 70–76.

767 Liang, X., Zhang, L., Natarajan, S.K., and Becker, D.F. (2013) Proline mechanisms of stress survival.
768 *Antioxid. Redox Signal.* **19**: 998–1011.

769 Ling, M., Allen, S.W., and Wood, J.M. (1994) Sequence Analysis Identifies the Proline Dehydrogenase
770 and Δ1-Pyrroline-5-carboxylate Dehydrogenase Domains of the Multifunctional *Escherichia coli*
771 PutA Protein. *J. Mol. Biol.* **243**: 950–956.

772 Liu, C., Wang, W., Wu, Y., Zhou, Z., Lai, Q., and Shao, Z. (2011) Multiple alkane hydroxylase systems
773 in a marine alkane degrader, *Alcanivorax dieselolei* B-5. *Environ. Microbiol.* **13**: 1168–1178.

774 Liu, H., Sun, W.-B., Liang, R.-B., Huang, L., Hou, J.-L., and Liu, J.-H. (2015) iTRAQ-based quantitative
775 proteomic analysis of *Pseudomonas aeruginosa* SJTD-1: A global response to *n*-octadecane
776 induced stress. *J. Proteomics* **123**: 14–28.

777 Lo Piccolo, L., De Pasquale, C., Fodale, R., Puglia, A.M., and Quatrini, P. (2011) Involvement of an
778 Alkane Hydroxylase System of *Gordonia* sp. Strain SoCg in Degradation of Solid *n* -Alkanes.
779 *Appl. Environ. Microbiol.* **77**: 1204–1213.

780 Lozada, M., Marcos, M.S., Commendatore, M.G., Gil, M.N., and Dionisi, H.M. (2014) The bacterial
781 community structure of hydrocarbon-polluted marine environments as the basis for the
782 definition of an ecological index of hydrocarbon exposure. *Microbes Environ.* **29**: 269–76.

783 Luan, X., Cui, Z., Gao, W., Li, Q., Yin, X., and Zheng, L. (2014) Genome Sequence of the Petroleum
784 Hydrocarbon-Degrading Bacterium *Alcanivorax* sp. Strain 97CO-5. *Genome Announc.* **2**:.

785 Marín, M.M., Smits, T.H., van Beilen, J.B., and Rojo, F. (2001) The alkane hydroxylase gene of
786 *Burkholderia cepacia* RR10 is under catabolite repression control. *J. Bacteriol.* **183**: 4202–9.

787 Marín, M.M., Yuste, L., and Rojo, F. (2003) Differential expression of the components of the two
788 alkane hydroxylases from *Pseudomonas aeruginosa*. *J. Bacteriol.* **185**: 3232–7.

789 Marquez, M.C. and Ventosa, A. (2005) *Marinobacter hydrocarbonoclasticus* Gauthier et al. 1992 and
790 *Marinobacter aquaeolei* Nguyen et al. 1999 are heterotypic synonyms. *Int. J. Syst. Evol.*
791 *Microbiol.* **55**: 1349–1351.

792 Mason, O.U., Hazen, T.C., Borglin, S., Chain, P.S.G., Dubinsky, E.A., Fortney, J.L., et al. (2012)
793 Metagenome, metatranscriptome and single-cell sequencing reveal microbial response to
794 Deepwater Horizon oil spill. *ISME J.* **6**: 1715–1727.

795 McKew, B.A., Lefebvre, S.C., Achterberg, E.P., Metodieva, G., Raines, C.A., Metodiev, M. V., and
796 Geider, R.J. (2013) Plasticity in the proteome of *Emiliania huxleyi* CCMP 1516 to extremes of
797 light is highly targeted. *New Phytol.* **200**: 61–73.

798 Menzel, R. and Roth, J. (1981) Regulation of the genes for proline utilization in *Salmonella*
799 *typhimurium*: autogenous repression by the putA gene product. *J. Mol. Biol.* **148**: 21–44.

800 Moxley, M.A., Tanner, J.J., and Becker, D.F. (2011) Steady-state kinetic mechanism of the
801 proline:ubiquinone oxidoreductase activity of proline utilization A (PutA) from *Escherichia coli*.
802 *Arch. Biochem. Biophys.* **516**: 113–120.
803

804 Nagata, K., Nagata, Y., Sato, T., Fujino, M.A., Nakajima, K., and Tamura, T. (2003) L-Serine, D- and L-
805 proline and alanine as respiratory substrates of *Helicobacter pylori*: correlation between in vitro
806 and in vivo amino acid levels. *Microbiology* **149**: 2023–2030.

807 Nara, T., Kawagishi, I., Nishiyama, S., Homma, M., and Imae, Y. (1996) Modulation of the
808 Thermosensing Profile of the *Escherichia coli* Aspartate Receptor Tar by Covalent Modification
809 of Its Methyl-accepting Sites. *J. Biol. Chem.* **271**: 17932–17936.

810 Nie, Y., Liang, J.-L., Fang, H., Tang, Y.-Q., and Wu, X.-L. (2014) Characterization of a CYP153 alkane
811 hydroxylase gene in a Gram-positive Dietzia sp. DQ12-45-1b and its "team role" with alkW1 in
812 alkane degradation. *Appl. Microbiol. Biotechnol.* **98**: 163–73.

813 Nishiyama, S., Umemura, T., Nara, T., Homma, M., and Kawagishi, I. (1999) Conversion of a bacterial
814 warm sensor to a cold sensor by methylation of a single residue in the presence of an
815 attractant. *Mol. Microbiol.* **32**: 357–365.

816 Panasia, G. and Philipp, B. (2018) LaoABCR, a Novel System for Oxidation of Long-Chain Alcohols
817 Derived from SDS and Alkane Degradation in *Pseudomonas aeruginosa*. *Appl. Environ.*
818 *Microbiol.* **84**: e00626-18.

819 Parales, R.E. and Ditty, J.L. (2010) Chemotaxis. In, *Handbook of Hydrocarbon and Lipid Microbiology*.
820 Springer Berlin Heidelberg, Berlin, Heidelberg, pp. 1529–1543.

821 Parks, D.H., Rinke, C., Chuvochina, M., Chaumeil, P.-A., Woodcroft, B.J., Evans, P.N., et al. (2017)
822 Recovery of nearly 8,000 metagenome-assembled genomes substantially expands the tree of
823 life. *Nat. Microbiol.* **2**: 1533–1542.

824 Parrilli, E., De Vizio, D., Cirulli, C., and Tutino, M.L. (2008) Development of an improved
825 *Pseudoalteromonas haloplanktis* TAC125 strain for recombinant protein secretion at low
826 temperature. *Microb. Cell Fact.* **7**: 2.

827 Partridge, J.D., Nieto, V., and Harshey, R.M. (2015) A new player at the flagellar motor: FliL controls

828 both motor output and bias. *MBio* **6**: e02367.

829 Peel, M., Donachie, W., and Shaw, A. (1988) Temperature-dependent Expression of Flagella of
830 *Listeria manocytogenes* Studied by Electron Microscopy, SDS-PAGE and Western Blotting.
831 *Microbiology* **134**: 2171–2178.

832 Phadtare, S. and Inouye, M. (2004) Genome-Wide Transcriptional Analysis of the Cold Shock
833 Response in Wild-Type and Cold-Sensitive, Quadruple-csp-Deletion Strains of *Escherichia coli. J.*
834 *Bacteriol.* **186**: 7007.

835 Porter, S.L., Wadhams, G.H., and Armitage, J.P. (2011) Signal processing in complex chemotaxis
836 pathways. *Nat. Rev. Microbiol.* **9**: 153–165.

837 Prabagaran, S.R., Manorama, R., Delille, D., and Shivaji, S. (2007) Predominance of *Roseobacter*,
838 *Sulfitobacter, Glaciecola and Psychrobacter* in seawater collected off Ushuaia, Argentina, Sub-
839 Antarctica. *FEMS Microbiol. Ecol.* **59**: 342–355.

840 Prud'homme-Généreux, A., Beran, R.K., Iost, I., Ramey, C.S., Mackie, G.A., and Simons, R.W. (2004)
841 Physical and functional interactions among RNase E, polynucleotide phosphorylase and the
842 cold-shock protein, CsdA: evidence for a 'cold shock degradosome.' *Mol. Microbiol.* **54**: 1409–
843 1421.

844 Ramakrishnan, R., Schuster, M., and Bourret, R.B. (1998) Acetylation at Lys-92 enhances signaling by
845 the chemotaxis response regulator protein CheY. *Proc. Natl. Acad. Sci. U. S. A.* **95**: 4918–23.

846 Ratajczak, A., Geissdörfer, W., and Hillen, W. (1998) Alkane hydroxylase from *Acinetobacter* sp.
847 strain ADP1 is encoded by alkM and belongs to a new family of bacterial integral-membrane
848 hydrocarbon hydroxylases. *Appl. Environ. Microbiol.* **64**: 1175–9.

849 Ratkowsky, D.A., Lowry, R.K., McMeekin, T.A., Stokes, A.N., and Chandler, R.E. (1983) Model for
850 bacterial culture growth rate throughout the entire biokinetic temperature range. *J. Bacteriol.*
851 **154**: 1222–6.

852 Rojo, F. (2009) Degradation of alkanes by bacteria. *Environ. Microbiol.* **11**: 2477–90.

853 Röling, W.F.M. and van Bodegom, P.M. (2014) Toward quantitative understanding on microbial
854 community structure and functioning: a modeling-centered approach using degradation of
855 marine oil spills as example. *Front. Microbiol.* **5**: 125.

856 Sagi, Y., Khan, S., and Eisenbach, M. (2003) Binding of the Chemotaxis Response Regulator CheY to
857 the Isolated, Intact Switch Complex of the Bacterial Flagellar Motor. *J. Biol. Chem.* **278**: 25867–
858 25871.

859 Schneiker, S., Martins dos Santos, V.A.P., Bartels, D., Bekel, T., Brecht, M., Buhrmester, J., et al.
860 (2006) Genome sequence of the ubiquitous hydrocarbon-degrading marine bacterium
861 *Alcanivorax borkumensis*. *Nat. Biotechnol.* **24**: 997–1004.

862 Sillitoe, I., Lewis, T.E., Cuff, A., Das, S., Ashford, P., Dawson, N.L., et al. (2015) CATH: comprehensive
863 structural and functional annotations for genome sequences. *Nucleic Acids Res.* **43**: D376–
864 D381.

865 Singh, S.K., Kotakonda, A., Kapardar, R.K., Kankipati, H.K., Sreenivasa Rao, P., Sankaranarayanan,
866 P.M., et al. (2015) Response of bacterioplankton to iron fertilization of the Southern Ocean,
867 Antarctica. *Front. Microbiol.* **6**: 863.

868 Soutourina, O.A., Semenova, E.A., Parfenova, V. V, Danchin, A., and Bertin, P. (2001) Control of
869 bacterial motility by environmental factors in polarly flagellated and peritrichous bacteria
870 isolated from Lake Baikal. *Appl. Environ. Microbiol.* **67**: 3852–9.

871 Strocchi, M., Ferrer, M., Timmis, K.N., and Golyshin, P.N. (2006) Low temperature-induced systems
872 failure in *Escherichia coli*: insights from rescue by cold-adapted chaperones. *Proteomics* **6**: 193–
873 206.

874 Takabe, K., Tahara, H., Islam, M.S., Affroze, S., Kudo, S., and Nakamura, S. (2017) Viscosity-
875 dependent variations in the cell shape and swimming manner of Leptospira. *Microbiology* **163**:

153–160.

Takekawa, N., Isumi, M., Terashima, H., Zhu, S., Nishino, Y., Sakuma, M., et al. (2019) Structure of Vibrio FliL, a New Stomatin-like Protein That Assists the Bacterial Flagellar Motor Function.

Tani, A., Ishige, T., Sakai, Y., and Kato, N. (2001) Gene structures and regulation of the alkane hydroxylase complex in *Acinetobacter* sp. strain M-1. *J. Bacteriol.* **183**: 1819–23.

Tanner, J.J. (2008) Structural biology of proline catabolism. *Amino Acids* **35**: 719–730.

Techtmann, S.M., Zhuang, M., Campo, P., Holder, E., Elk, M., Hazen, T.C., et al. (2017) Corexit 9500 Enhances Oil Biodegradation and Changes Active Bacterial Community Structure of Oil-Enriched Microcosms. *Appl. Environ. Microbiol.* **83**: e03462-16.

Throne-Holst, M., Wentzel, A., Ellingsen, T.E., Kotlar, H.-K., and Zotchev, S.B. (2007) Identification of Novel Genes Involved in Long-Chain *n*-Alkane Degradation by *Acinetobacter* sp. Strain DSM 17874. Appl. Environ. Microbiol. 73: 3327–3332.

Tipping, M.J., Delalez, N.J., Lim, R., Berry, R.M., and Armitage, J.P. (2013) Load-dependent assembly of the bacterial flagellar motor. *MBio* **4**: e00551-13.

Turner, L., Caplan, S.R., and Berg, H.C. (1996) Temperature-induced switching of the bacterial flagellar motor. *Biophys. J.* **71**: 2227–2233.

Veillette, J., Lovejoy, C., Potvin, M., Harding, T., Jungblut, A.D., Antoniades, D., et al. (2011) Milne Fiord epishelf lake: A coastal Arctic ecosystem vulnerable to climate change. *Écoscience* **18**: 304–316.

Wadhams, G.H. and Armitage, J.P. (2004) Making sense of it all: bacterial chemotaxis. *Nat. Rev. Mol. Cell Biol.* **5**: 1024–1037.

Wadhawan, S., Gautam, S., and Sharma, A. (2014) Involvement of proline oxidase (PutA) in programmed cell death of *Xanthomonas*. *PLoS One* **9**: e96423.

900 Wang, L., Wang, W., Lai, Q., and Shao, Z. (2010) Gene diversity of CYP153A and AlkB alkane
901 hydroxylases in oil-degrading bacteria isolated from the Atlantic Ocean. *Environ. Microbiol.* **12**:
902 1230–1242.

903 Wang, W. and Shao, Z. (2013) Enzymes and genes involved in aerobic alkane degradation. *Front.*
904 *Microbiol.* **4**: 116.

905 Wang, W. and Shao, Z. (2014) The long-chain alkane metabolism network of *Alcanivorax dieselolei*.
906 *Nat. Commun.* **5**: 5755.

907 Wang, Y., Yu, M., Austin, B., and Zhang, X.-H. (2012) *Oleispira lenta* sp. nov., a novel marine
908 bacterium isolated from Yellow sea coastal seawater in Qingdao, China. *Antonie Van*
909 *Leeuwenhoek* **101**: 787–794.

910 Whyte, L.G., Smits, T.H.M., Labbé, D., Witholt, B., Greer, C.W., and van Beilen, J.B. (2002) Gene
911 cloning and characterization of multiple alkane hydroxylase systems in *Rhodococcus* strains
912 Q15 and NRRL B-16531. *Appl. Environ. Microbiol.* **68**: 5933–42.

913 Wolfe, A.J. (2005) The Acetate Switch. *Microbiol. Mol. Biol. Rev.* **69**: 12–50.

914 Wösten, M.M.S.M., van Dijk, L., Veenendaal, A.K.J., de Zoete, M.R., Bleumink-Pluijm, N.M.C., and van
915 Putten, J.P.M. (2010) Temperature-dependent FlgM/FliA complex formation regulates
916 *Campylobacter jejuni* flagella length. *Mol. Microbiol.* **75**: 1577–1591.

917 Yakimov, M.M., Giuliano, L., Denaro, R., Crisafi, E., Chernikova, T.N., Abraham, W.-R., et al. (2004)
918 *Thalassolituus oleivorans* gen. nov., sp. nov., a novel marine bacterium that obligately utilizes
919 hydrocarbons. *Int. J. Syst. Evol. Microbiol.* **54**: 141–8.

920 Yakimov, M.M., Giuliano, L., Gentile, G., Crisafi, E., Chernikova, T.N., Abraham, W.-R., et al. (2003)
921 *Oleispira antarctica* gen. nov., sp. nov., a novel hydrocarbonoclastic marine bacterium isolated
922 from Antarctic coastal sea water. *Int. J. Syst. Evol. Microbiol.* **53**: 779–85.

Yakimov, M.M., Golyshin, P.N., Lang, S., Moore, E.R., Abraham, W.R., Lünsdorf, H., and Timmis, K.N. (1998) *Alcanivorax borkumensis* gen. nov., sp. nov., a new, hydrocarbon-degrading and surfactant-producing marine bacterium. *Int. J. Syst. Bacteriol.* **48 Pt 2**: 339–48.

Yin, X., Luan, X., Xu, A., Li, Q., Cui, Z., and Valentine, D.L. (2018) Genome Sequence of a Marine Alkane Degrader, *Alcanivorax* sp. Strain 97CO-6. *Genome Announc.* **6**:.

Zhang, Y. (2008) I-TASSER server for protein 3D structure prediction. *BMC Bioinformatics* **9**: 40.

Zhang, L., Alfano, J.R., and Becker, D.F. (2015) Proline metabolism increases katG expression and oxidative stress resistance in Escherichia coli. *J. Bacteriol.* **197**: 431–40.

Zhao, R., Collins, E.J., Bourret, R.B., and Silversmith, R.E. (2002) Structure and catalytic mechanism of the E. coli chemotaxis phosphatase CheZ. *Nat. Struct. Biol.* **9**: 570–5.

Zybailov, B., Mosley, A.L., Sardiu, M.E., Coleman, M.K., Florens, L., and Washburn, M.P. (2006) Statistical Analysis of Membrane Proteome Expression Changes in *Saccharomyces c erevisiae*. *J. Proteome Res.* **5**: 2339–2347.

945 **Figure 1**

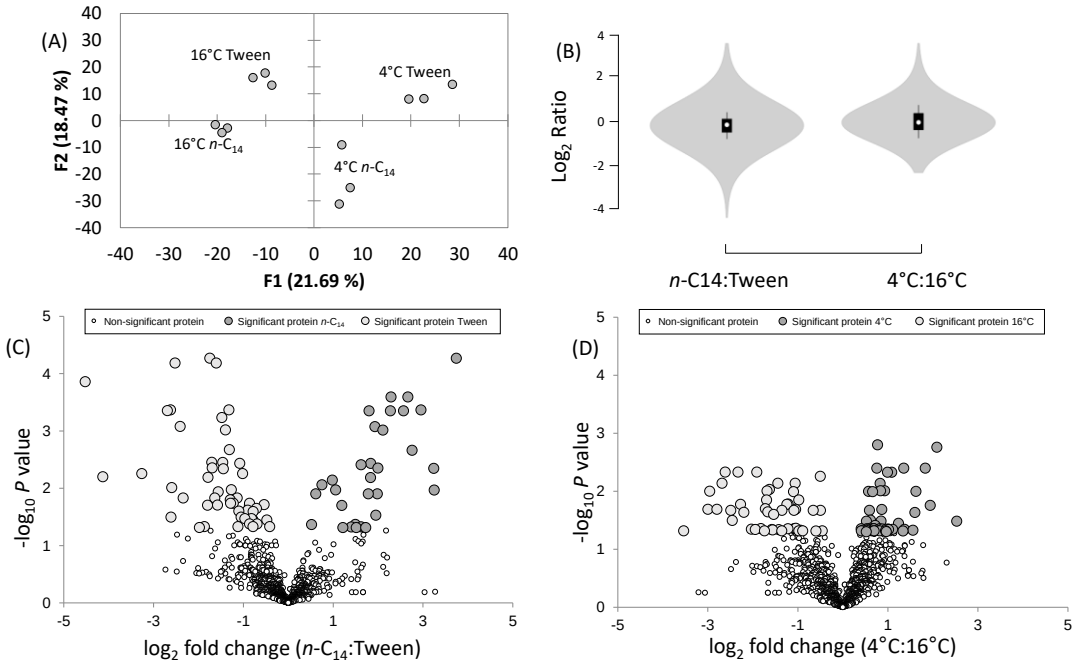

946

947

948

949

950

951

952

953

954

955

956

957

Figure 2

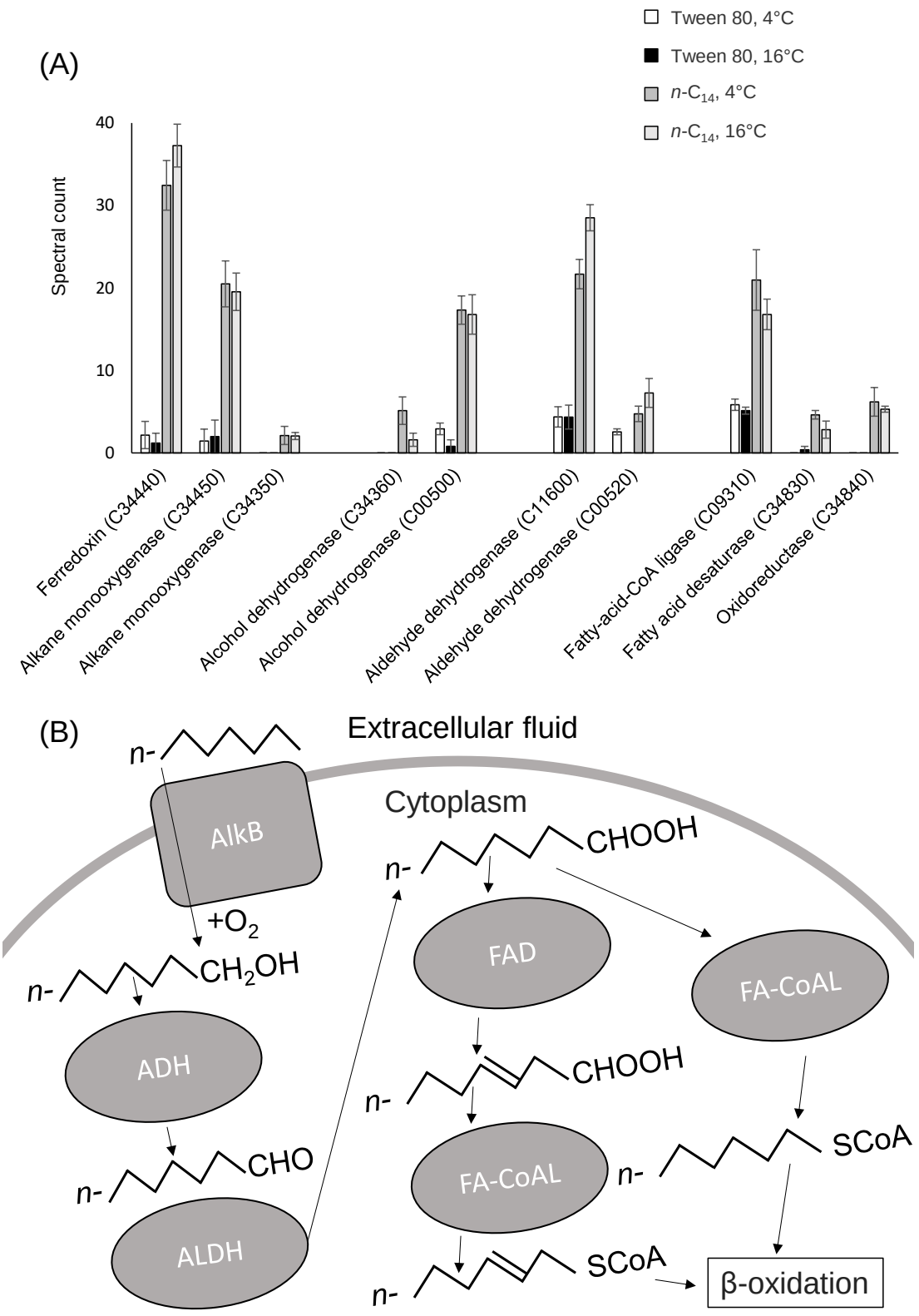
(A)
Tween 80, 4°C
Tween 80, 16°C
n-C14, 4°C
n-C14, 16°C
Spectral count
40
30
20
10
0
Ferredoxin (C34440)
Alkane monooxygenase (C34450)
Alkane monooxygenase (C34350)
Alcohol dehydrogenase (C34360)
Alcohol dehydrogenase (C00500)
Aldehyde dehydrogenase (C11600)
Aldehyde dehydrogenase (C00520)
Fatty-acid-CoA ligase (C09310)
Fatty acid desaturase (C34830)
Oxidoreductase (C34840)
(B)
Extracellular fluid
Cytoplasm
n-
AlkB
+O2
CH2OH
ADH
CHO
ALDH
CHOOH
FAD
FA-CoAL
SCoA
β-oxidation

961 **Figure 3**

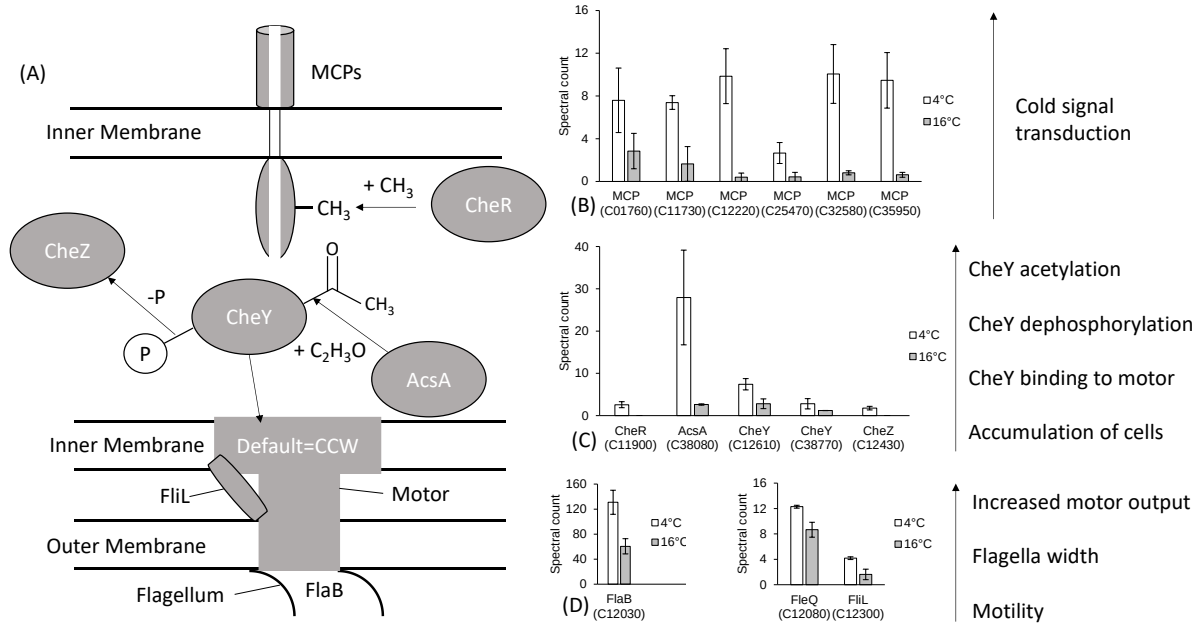

962

963 **Figure 4**

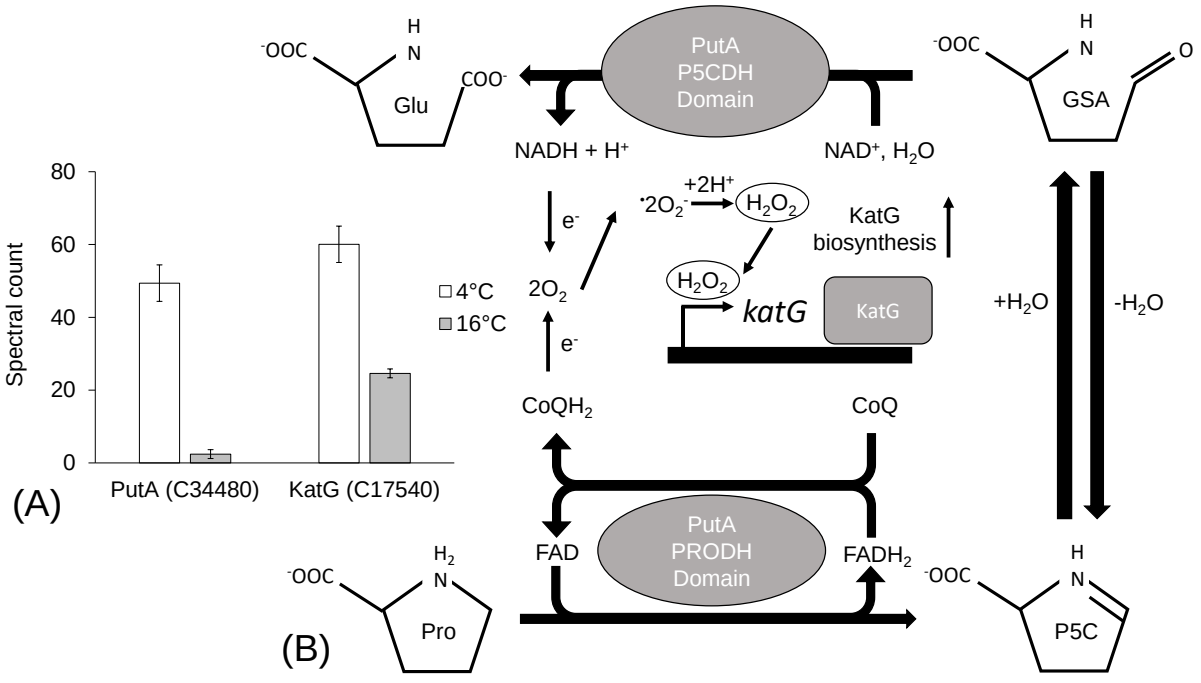

964